Int. J. Bio-Inorg. Hybr. Nanomater., Vol. 3, No. 2 (2014), 117-123
ISSN Print: 2251-8533
ISSN Online: 2322-4142

International Journal of Bio-Inorganic Hybrid Nanomaterials

Preparation and Utilization of MnO_2 Nanoparticles (NPs) Catalyst for the Decontamination against Chemical Warfare Nerve Agent Simulant (CWNAS)

Meysam Sadeghi[1*], Sina Yekta[2], Nooshin Shahabfar[3], Mirhassan Husseini[1], Hadi Adeli[2], Mohammad Javad Taghizadeh[4]

[1] M.Sc., Department of Chemistry, Faculty of Basic Sciences, Imam Hussein Comprehensive University (IHCU), Tehran, Iran

[2] M.Sc., Department of Chemistry, Faculty of Basic Sciences, Islamic Azad University, Qaemshahr Branch, Qaemshahr, Iran

[3] M.Sc., Department of Nuclear Engineering, Radiation Application, Amir Kabir University, Tehran, Iran

[4] Ph.D., Department of Chemistry, Faculty of Basic Sciences, Imam Hussein Comprehensive University (IHCU), Tehran, Iran

Received: 30 March 2014; Accepted: 3 June 2014

ABSTRACT

In this scientific research, MnO_2 nanoparticles (NPs) have been successfully prepared by a precipitation method using $KMnO_4$, $MnSO_4.H_2O$ and H_2O_2 (30%) as the precursors. As-prepared sample was identified by X-ray diffraction (XRD), Scanning electron microscopy (SEM), Transmission electron microscopy (TEM) and Infrared (IR) techniques. The transmission electron microscopy (TEM) showed 7-8 nm ranges size of as prepared MnO_2 nanoparticles. The decontamination reaction of triethyl phosphate (TEP) as a chemical warfare nerve agent simulant (CWNAS) was carried out on the surface of MnO_2 NPs as the sorbent catalyst with the different weight ratios of TEP/MnO_2 (1:8, 1:16 and 1:32) and studied by using phosphorous-31 nuclear magnetic resonance spectroscopy (^{31}PNMR) technique. The ^{31}PNMR analysis results proved that more than 95% of TEP was adsorbed on this catalyst in decane solvent with ratio of 1:32 after the elapse of the reaction time (8 h) at room temperature (25±1°C). On the other hand, decontaminated agent simulant amounts for the ratios of 1:16 and 1:8 were lower under similar conditions, respectively. This sorbent catalyst provides enough surface area and enhanced chemical reactivity for instantaneous adsorption and decontamination of TEP.

Keyword: MnO_2 Nanoparticles (NPs); Precipitation; Catalyst; Decontamination; Nerve agent simulant; Triethyl phosphate (TEP); Adsorption.

1. INTRODUCTION

Chemical weapons are considered as weapons of mass destruction (WMD). Under the Chemical Weapons Convention, chemical weapons are defined as munitions and devices specifically designed to cause death or other harm through the release of toxic chemicals or precursors for toxic chemicals as a result of the em-

(*) Corresponding Author - e-mail: meysamsadeghi45@yahoo.com

ployment of such weapons [1]. A toxic chemical is defined as any chemical which through its chemical action on life processes can cause death, temporary incapacitation or permanent harm to humans or animals. A precursor for a toxic chemical is defined as any chemical reactant which takes part at any stage in the production of a toxic chemical. This includes any key component of a binary or multicomponent chemical system [2, 3]. Such toxic chemicals are often called chemical warfare agents (CWA). Chemical warfare agents are often categorized in accordance with their physiological mode of operation: nerve, blister, choking, blood, and incapacitating agents.

Nerve agents are a subfamily of organophosphorus compounds developed for chemical warfare. Most of the nerve agents were originally synthesized in a search for insecticides, but because of their toxicity, they were evaluated for military use [3]. These agents, are often called "anticholinesterases", because they phosphoryle the enzyme acetylcholinesterase (AChE), which plays a significant role in the nervous system. Before going into the details of how nerve agents inhibit this enzyme, it is important to understand the role of this enzyme in the nervous system, which is explained below [4-6]. The triethyl phosphate (TEP) is frequently used as a simulant molecule for understanding the activity of the organophosphorus nerve agents (G-agents), since it is nontoxic and exhibits structural similarities to the nerve agents (Scheme 1). Moreover, TEP exhibits many of the group frequencies associated with the actual agents in infrared spectroscopy, making it ideal for evaluating infrared methods of nerve agent detection [7].

Although it is not classified as toxic, it is harmful if inhaled, swallowed, or absorbed through the skin. The different materials such as bleach, hydrogen peroxide, DS2, etc., were applied for the decontamination of these compounds [7]. Certain disadvantages exist with the use of these adsorbents such as environmental contaminates. For this purpose, the solid adsorbents were utilized.

Among them, Metal oxides reveal superior ability to adsorb chemical warfare agent (CWA) compared to pure metal surfaces. This is often attributed to reactive sites on the surface of metal oxide through which organophosphonate species (nerve agents) can adsorb and subsequently undergo a hydrolysis reaction. A wide variety of metal oxide systems have been studied, from clean, crystalline surfaces to high surface area nanomaterials. Metal oxides, well known for their industrial use as adsorbents, catalysts and catalyst supports, have several potential decontamination applications such as environment friendly hasty decontamination on the battlefield, protective filtration systems for vehicles, aircraft, and buildings, and the demilitarization of CWA munitions and stockpiles. In contrast to their conventional counterparts, nanoscale metal oxides possess significantly different properties and have been established as the potential adsorbent materials for decontamination of CWA. Metal oxides, such as MgO [8, 9], CaO [10, 11], Al_2O_3 [12-16], TiO_2 [17-26], ZnO [27-29], etc., are currently under consideration as destructive adsorbents for decontamination of CWA. In this research, for the first time, the decontamination TEP was investigated on the MnO_2 nanoparticles (NPs) at room temperature.

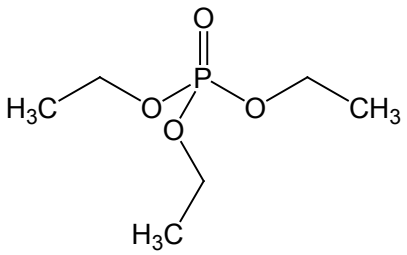

Scheme 1: *Molecular structure of triethyl phosphate (TEP).*

2. EXPERIMENTAL

2.1. Materials

$KMnO_4$, $MnSO_4.H_2O$, H_2O_2 (30%), phosphoric acid, decane and $CDCl_3$ were purchased from Merck Co. (Germany). Triethyl phosphate (TEP) form Sigma–Aldrich Co. (USA) was used as received. Distilled water was also used as the solvent in the experiment.

2.2. Characterization process and of instruments

The X-ray diffraction (XRD) analysis was carried out on a Philips X-ray diffractometer using CuKα radiation (40 kV, 30 mA and λ= 0.15418 nm). Sample were scanned at 2°/min in the range of 2theta (2θ) = 1070°. The morphology of the sample was recorded using Scanning Electron Microscope Spectroscopy

(SEM, LEO-1530VP). Transmission electron microscope (TEM) image were taken on a FEI Tecnai G2 20 S-TWIN. The IR spectrum was scanned using a Perkin-Elmer FTIR (Model 2000) in the wavelength range of 450 to 4000 cm^{-1} with KBr pellets method. In order to investigate the reaction of the nerve agent simulant with the catalyst, phosphorous-31 nuclear magnetic resonance spectroscopy (^{31}PNMR, Bruker 250 MHz) and centrifuge (Universal, CAT. NO. 1004) instruments were used.

2.3. Preparation of MnO_2 nanoparticles (NPs)

For this purpose, 3.2 g of $KMnO_4$ and 1.75 g of $MnSO_4.H_2O$ were mixed and dissolved at room temperature in 75 mL of H_2O_2 solution (1:1 molar ratios of H_2O_2 to distilled water) via magnetic stirring to form a homogeneous solution. When the mixed solution changed to a dark brown gel-like solution, it was immediately transferred to the autoclave, sealed and heated at 180°C for 3 h. After the reaction was complete, the reactor was taken out and naturally cooled to room temperature. The resulting brown-black precipitates were filtered off, washed with distilled water several times to remove excess ions, and finally dried at 120°C in air overnight.

2.4. Decontamination reaction procedure of the nerve agent simulant on the MnO_2 NPs catalyst

Sample preparation meets four steps: (1) 0.03 M phosphoric acid (H_3PO_4) as the blank solution was prepared through dilution of 0.05 mL of H_3PO_4 with 25 mL of deionized water. This blank solution was injected to a capillary column whose tips were closed by heat (S1). (2) Nerve agent simulant solutions were prepared through addition of 10 μL of TEP to 10 mL of decane as solvent (S2). (3) S2 solutions were mixed separately with 0.12, 0.24 and 0.48 g of MnO_2 NPs in three 50 mL Erlenmeyer flasks and stirred vigorously for 8 h at room temperature (S3). (4) 1 mL of each one of S3 mixtures was placed in centrifuge tubes and centrifuged at 500 rpm for 4 min. Afterward, 0.3 mL of the above samples and 0.1 mL of $CDCl_3$ were added to NMR tubes along with the capillary column (S1 solution sample) as the blank solution. Finally, the presence of TEP in the sample was revealed by ^{31}PNMR analysis.

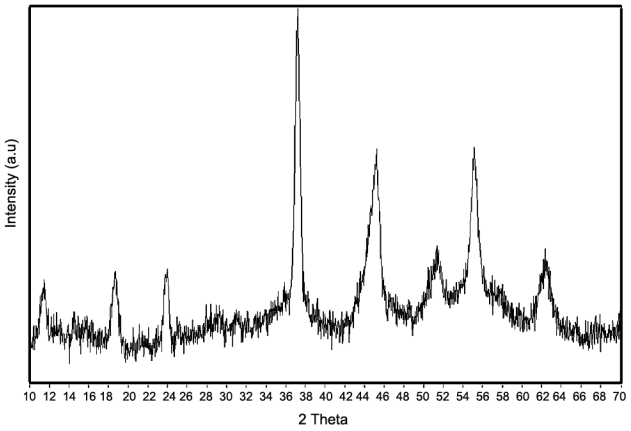

Figure 1: *XRD patterns of synthesized MnO_2 NPs.*

3. RESULTS AND DISCUSSION

3.1. XRD study

The structure of the MnO_2 catalyst has been assayed by X-ray diffraction patterns is shown in Figure 1. The crystalline size was determined from full width at half maximum (FWHM) parameter with the most intense peak obtained in XRD patterns. The average particle size of MnO_2 nanoparticles was calculated from line broadening of the peak at 2θ = 10-70° using Debye-Scherrer formula:

$$d = \frac{0.94\lambda}{\beta \cos\theta} \quad (1)$$

Where d is the crystalline size, λ is the wavelength of X-ray Cu Kα source (= 1.54056 Å), β is the full width at half maximum (FWHM) of the most predominant peak at 100% intensity and θ is Bragg diffraction angle at which the peak is recorded. No characteristic peaks

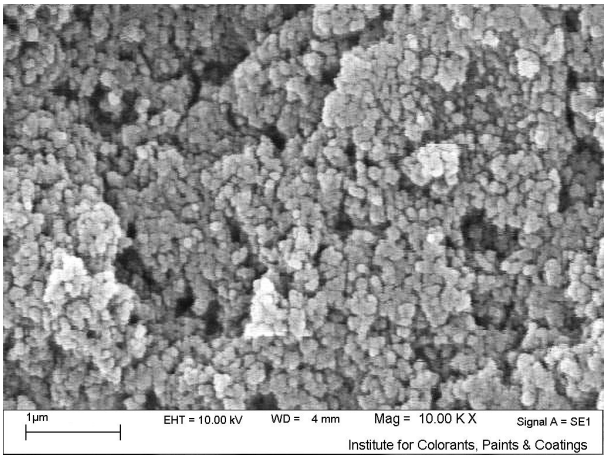

Figure 2: *SEM image of synthesized MnO_2 NPs.*

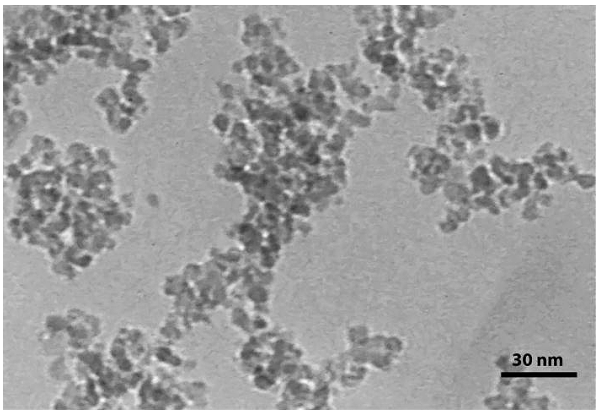

Figure 3: *TEM image of synthesized MnO_2 NPs.*

corresponded to the impurity were found, confirming that high-purity products be obtained. In two of the XRD patterns, seven peaks were revealed at approximately 2θ = 11.6, 18.4, 23.6, 37.3, 44.2, 51.5, 55.3 and 62.3, which correspond to the Bragg's reflection plane (1 1 0), (2 0 0), (3 1 0), (1 3 1), (3 0 0), (4 1 1), (1 6 0) and (5 2 1) for MnO_2 nanoparticles, respectively. Using this formula, the smaller average particle sizes by Debye-Scherrer formula were estimated to be 7.3 nm for MnO_2 nanoparticles.

3.2. SEM and TEM studies

The SEM micrograph of manganese dioxide (MnO_2) nanaoparticles for the investigation of the morphology and structure is shown in Figure 2. The results have emphasized that this catalyst have nano-sized particles. Also, Figure 3 shows the TEM image of as prepared nanoparticles. The size of particle observed in TEM image is in the range of 7-8 nm which is in good agreement with calculated by Scherrer formula using XRD.

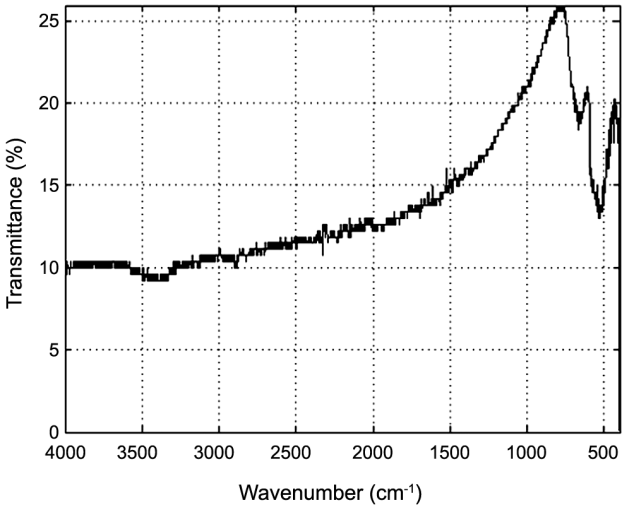

Figure 4: *IR spectrum of synthesized MnO_2 NPs.*

3.3. IR study

The IR spectrum of the nanoparticles is shown in Figure 4. The peaks at 560 and 670 cm^{-1} are corresponded to the Mn-O bonds. Also, the peak at 3450 cm^{-1} is related to the adsorbed water on the surface of synthesized MnO_2 nanoparticles.

3.4. ^{31}PNMR analysis

The decontamination reaction of TEP was accomplished at room temperature (25±1°C) and decane solvent using ^{31}P nuclear magnetic resonance (^{31}PNMR) as a rapid and suitable analytical technique. The quantitative works of ^{31}PNMR spectroscopy were performed in the presence of phosphoric acid (H_3PO_4) as a suitable inorganic internal standard for the determination of reaction efficiency. To investigate the amount percent of agent simulant neutralized, the under peak integral two sample of TEP and H_3PO_4 for the different weight ratios of 1:8, 1:16 and 1:32 were given. Then, the ratio of agent simulant integral to H_3PO_4 (agent simulant integral/H_3PO_4 integral) was determined. ^{31}PNMR spectra and data results are shown in Figure 5 and Table 1. It can be seen from the spectra, two signals were revealed. A narrow peak at around approximately δ= 32 ppm corresponded to the chemical shift of TEP and the characteristic sharp peak at around δ= 0 (zero) ppm also related to the phosphoric acid (H_3PO_4) as the blank solution.

The obtained results denoted that with increasing the reaction ratio of TEP/MnO_2 NPs, the higher amount of TEP was neutralized while in the time after 8 h, more than 95% this agent simulant was adsorbed for the ratio of 1:32. On the other hand, the ratios of 1:16 and 1:8 have the lower results under similar conditions, respectively.

3.5. Mechanism of the decontamination procedure

After the investigation of the reaction between TEP and MnO_2 nanoparticles sorbent catalyst, a mechanism scheme reflecting the decontamination process is proposed upon which a route along with the roles of manganese dioxide-diethyl phosphate (MnO_2-DEP) and manganese dioxide-ethyl phosphate (MnO_2-EP)

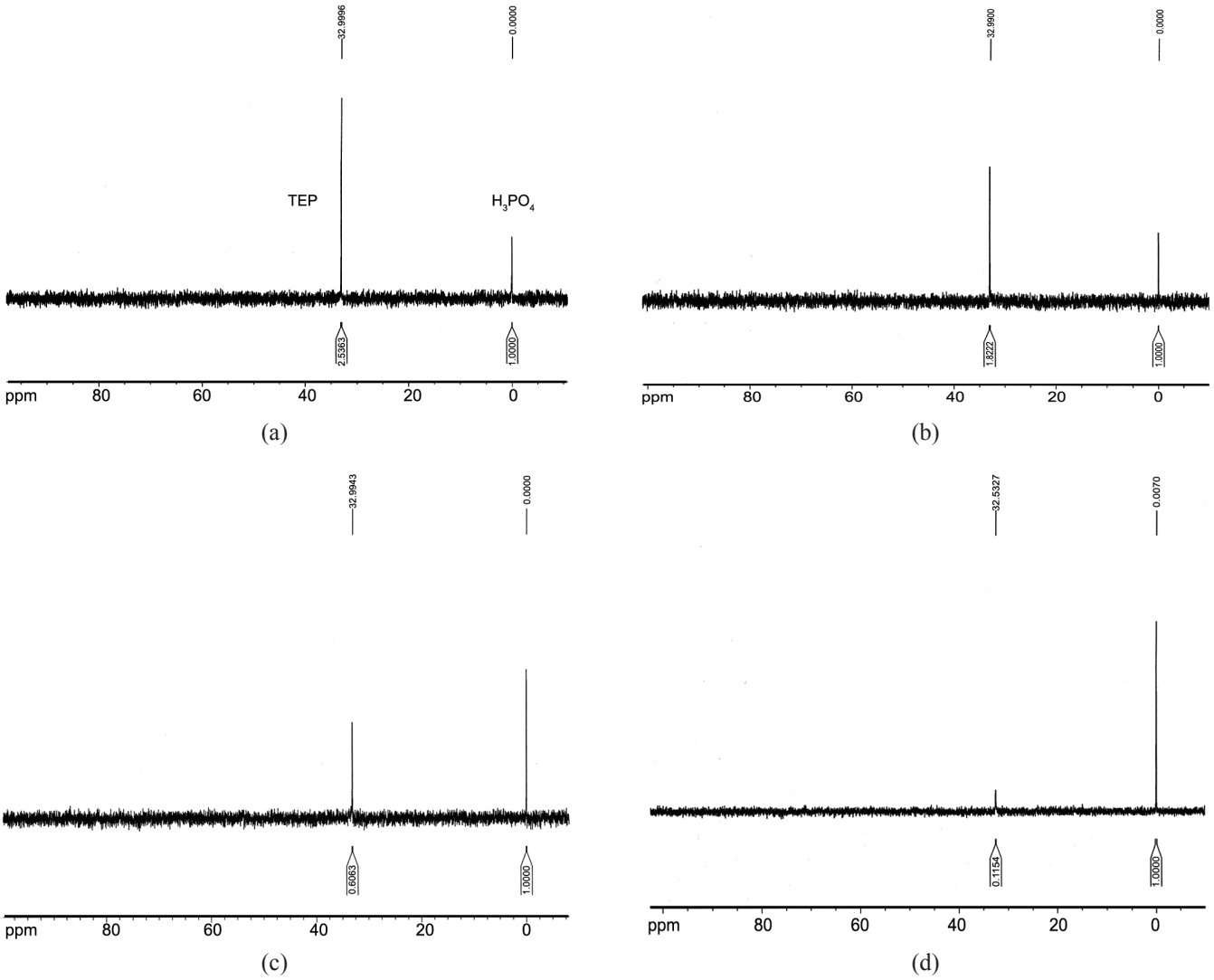

Figure 5: *^{31}PNMR spectra for the adsorption of TEP on the MnO_2 nanoparticles in decane solvent.*

as intermediates, the subsequent cleavage of the P–O bonds in TEP and the formation diethyl phosphonic and ethyl phosphonic as the products, are predicted (Schemes 2). TEP molecule contains bivalent oxygen atom which possesses two lone pairs of electrons. In this route, TEP molecule reacts with Lewis acid sites (Mn^{4+}) and Bronsted acid sites (hydroxyl groups (Mn-OH)) presented on the surface of the catalyst through two phosphoryl oxygen and two manganese atoms to form surface bound Mn-O-P-O-Mn and P-$(O\text{-}Mn)_3$ species. In these interactions, methoxy groups to be removed. On the other hand, these products were not

Table 1: *^{31}PNMR spectra results for TEP/MnO_2 nanoparticles samples in decane solvent.*

TEP Intg	phosphoric acid blank Intg	TEP Intg/ phosphoric acid blank Intg	TEP Concentration % (M)	decontaminated TEP %	Ratio	Sample
2.5363	1.0000	2.5363	0.0300	00.00	1:0	a
1.8222	1.0000	1.8222	0.0215	28.15	1:8	b
0.6063	1.0000	0.6063	0.0071	76.09	1:16	c
0.1154	1.0000	0.1154	0.0013	95.44	1:32	d

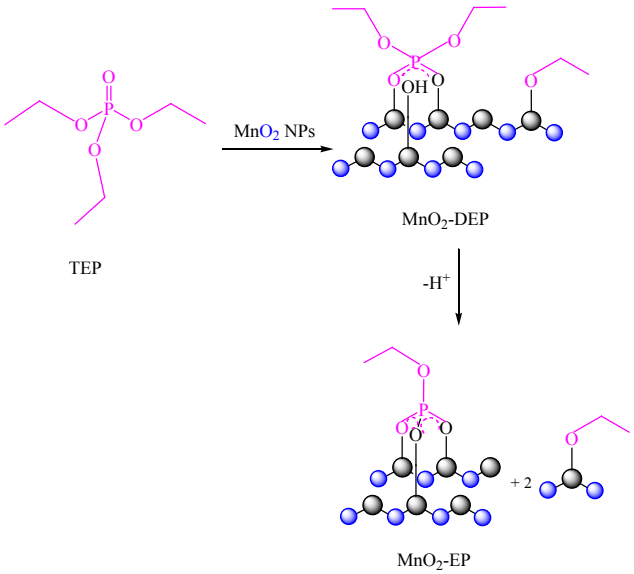

Scheme 2: *Adsorption pathway for TEP on the MnO_2 involving Mn^{4+} Lewis acid sites and Bronsted (hydroxyl groups (Mn-OH)) sites.*

observed from the ^{31}PNMR spectra because adsorbed on the surface of MnO_2 nanoparticles.

4. CONCLUSIONS

In summary, first, MnO_2 nanoparticles were synthesized by precipitation method and characterized. Then, the synthesized nanoparticles were employed as catalyst for the decontamination against TEP as toxic organophosphorous nerve agent simulants. On the basis of the above investigations, MnO_2 NPs have a high catalytic potential for the adsorption of this agent simulant and a high potential for instantaneous adsorption and decontamination of chemical warfare nerve agent simulant.

ACKNOWLEDGEMENTS

The authors thank Department of chemistry, Faculty of Science of Imam Hussein Comprehensive University (IHCU), Tehran for all supports provided.

REFERENCES

1. Szinicz L., *Toxicology*, **214** (2005), 167.
2. Diab M.Z., *The Nonproliferation Review*, **5** (1997), 104.
3. Talmage S.S., Watson A.P., Hauschild V., Munro N.B., King J., *Curr. Org. Chem.*, **11** (2007), 285.
4. Bartelt-Hunt S.L., Knappe D.R.U., Barlaz M.A., *Crit. Rev. Env. Sci. Tec.*, **38** (2008), 112.
5. Corbridge D., *Biochem. Technol. Elsevier: Amsterdam*, **6** (1976), 319.
6. J. Emsley, D. Hall, 1976. *The Chemistry of Phosphorus*, Harper & Row: New York.
7. Bertilsson L., Potje-Kamloth K., Liess H.D., Engquist I., *Liedberg B. J. Phys. Chem. B*, **102** (1998), 1260.
8. Michalkova A., Ilchenko M., Gorb L., Leszczynski J., *J. Phys. Chem. B*, **108** (2004), 5294.
9. Wagner G.W., Bartram P.W., Koper O., Klabunde K.J., *J. Phys. Chem.*, **103** (1999), 3225.
10. Michalkova A., Paukku Y., Majumdar D., *J. Chem. Phys. Lett.*, **72** (2007), 438.
11. Wagner G.W., Koper O.B., Lucas E., Decker S., Klabunde K.J., *J. Phys. Chem.*, **104** (2000), 5118.
12. Kuiper A.E.T., Bokhoven J.J.G.M., Medema J., *J. Catal.*, **43** (1976), 154.
13. Saxena A., Singh B., Srivastava A.K., Suryanarayana M.V.S., Ganesan, K., Vijayaraghavan R., Dwivedi K.K., *Micropor. Mesopor. Mater*, **115** (2008), 364.
14. Saxena A., Sharma A., Srivastava A.K., Singh B., Gutch P.K., Semwal R.P., *J. Chem. Technol. Biotechnol.*, **84** (2009), 1860.
15. Saxena A., Srivastava A.K., Singh B., Gupta A.K., Suryanarayana M.V.S., Pandey P., *J. Hazard. Mater*, **175** (2010), 795.
16. Wagner G.W., Procell L.R., O'Connor R.J., Munavalli S., Carnes C.L., Kapoor P.N., Klabunde K.J., *J. Am. Chem. Soc.*, **123** (2001), 1636.
17. Hirakawa T., Sato K., Komano A. Kishi S., Nishimoto C.K., Mera N., Kugishima M., Sano T., Ichinose H., Negishi N., Seto Y., Takeuchi K., *J. Phys. Chem.*, **114** (2010), 2305.
18. Naseri M.T., Sarabadani M., Ashrafi D., Saeidian H., Babri M., *Environ. Sci. Pollut. Re.*, **20** (2012), 907.
19. Prasad G.K., Mahato T.H., Singh B., Ganesan K., Srivastava A.R., Kaushik M.P., Vijayaraghavan R., *AIChE J.*, **54** (2008), 2957.

20. Prasad G.K., Singh B., Ganesan K., Batra A., Kumeria T., Gutch, P.K. Vijayaraghavan, R., *J. Hazard. Mater*, **167** (2009), 1192.
21. Ramacharyulu P.V.R.K., Prasad G.K., Ganesan K., Singh B., *J. Mol. Catal. A: Chem.*, **132** (2012), 353.
22. Sato K., Hirakawa T., Komano A., Kishi S., Nishimoto C.K., Mera N., Kugishima M., Sano T., Ichinose H., Negishi N., Seto Y., Takeuchi K., Appl. Catal., *B: Environ*, **106** (2011), 316.
23. Stengl V., Maríkova M., Bakardjieva S., Subrt J., Oplustil F. Olsanska M., *J. Chem. Technol. Biotechnol*, **80** (2005), 754.
24. Stengl V., Grygara T.M., Oplustil F., Nemec T., *J. Hazard. Mater,* **62** (2012), 227.
25. Wagner G.W., Chen Q., Wu Y., *J. Phys. Chem. C*, **112** (2008), 11901.
26. Wagner G.W., Peterson G.W., Mahle J.J., *Ind. Eng. Chem. Res.*, **51** (2012), 3598.
27. Mahato T.H., Prasad G.K., Singh B., Acharya J., Srivastava A.R., Vijayaraghavan R., *J. Hazard. Mater*, **165** (2009), 928.
28. Prasad G.K., Mahato T.H., Singh B., Ganesan K., Pandey P., Sekhar K., *J. Hazard. Mater*, **149** (2007), 460.
29. Prasad G.K., Ramacharyulu P.V.R.K., Singh B., Batra K., Srivastava A.R., Ganesan K., Vijayaraghavan R., *J. Mol. Catal. A: Chem.*, **349** (2011), 55.